The Three-Dimensional Distribution of Clouds over the Southern Hemisphere High Latitudes

KATHRYN L. VERLINDEN, DAVID W. J. THOMPSON, AND GRAEME L. STEPHENS

Department of Atmospheric Science, Colorado State University, Fort Collins, Colorado

(Manuscript received 30 June 2010, in final form 13 April 2011)

ABSTRACT

The authors exploit three years of data from the *CloudSat* and Cloud–Aerosol Lidar and Infrared Pathfinder Satellite Observation (CALIPSO) satellites to document for the first time the seasonally varying vertical structure of cloudiness throughout Antarctica and the high-latitude Southern Ocean. The results provide a baseline reference of Southern Hemisphere high-latitude cloudiness for future observational and modeling studies, and they highlight several previously undocumented aspects and key features of Antarctic cloudiness.

The key features of high-latitude Southern Hemisphere cloudiness documented here include 1) a pronounced seasonal cycle in cloudiness over the high-latitude Southern Hemisphere, with higher cloud incidences generally found during the winter season over both the Southern Ocean and Antarctica; 2) two distinct maxima in vertical profiles of cloud incidence over the Southern Ocean, one centered near the surface and another centered in the upper troposphere; 3) a nearly discontinuous drop-off in cloudiness near 8 km over much of the continent that peaks during autumn, winter, and spring; 4) large east–west gradients in upper-level cloudiness in the vicinity of the Antarctic Peninsula that peak during the austral spring season; and 5) evidence that cloudiness in the polar stratosphere is marked not by a secondary maximum at stratospheric levels but by a nearly monotonic decrease with height from the tropopause.

Key results are interpreted in the context of the seasonally varying profiles of vertical motion and static stability and compared with results of previous studies.

1. Introduction

Understanding the observed distribution of tropospheric clouds over the high latitudes of the Southern Hemisphere is important for a variety of reasons. The space/time distribution of clouds plays a key role in the surface and atmospheric energy budget of polar regions (e.g., Kay et al. 2008). An accurate characterization of Antarctic cloudiness is required to test the ability of general circulation models to simulate the climate of the Southern Hemisphere polar regions. Understanding the current distribution of high-latitude Southern Hemisphere cloudiness is a prerequisite for predicting future changes in Antarctic climate.

However, the seasonally varying vertical structure of cloudiness over the high latitudes of the Southern Hemisphere remains largely unknown. In situ measurements of clouds are available at only a few locations over Antarctica (e.g., Mahesh et al. 2001; Lachlan-Cope et al. 2001; Town et al. 2007) and are largely absent over the Southern Ocean. Spaceborne instruments such as the Advanced Very High Resolution Radiometer (AVHRR) provide continent-wide visible and infrared imagery of Antarctica (e.g., Yamanouchi and Kawaguchi 1992; Lubin and Harper 1996; Murata and Yamanouchi 1997; Hatzianastassiou et al. 2001; Turner et al. 2001; Pavolonis and Key 2003), and the seasonal cycle of zonal-mean high-latitude Southern Hemisphere cloudiness was explicitly calculated in Hatzianastassiou et al. (2001) and Pavolonis and Key (2003) based on such remotely sensed data. However, the AVHRR products have difficulty discerning between clouds and the surface over regions of snow and ice, provide very limited information on the vertical structure of cloudiness, and are not yet considered adequate for identifying clouds over the Antarctic Plateau (e.g., Town et al. 2007). The International Satellite Cloud Climatology Project (ISCCP) dataset uses AVHRR over polar regions and is thus similarly limited over the Antarctic (e.g., Town et al. 2007). The spaceborne

Corresponding author address: David W. J. Thompson, Department of Atmospheric Science, Colorado State University, 1371 Campus Delivery, Fort Collins, CO 80523-1371.
E-mail: davet@atmos.colostate.edu

DOI: 10.1175/2011JCLI3922.1

Geoscience Laser Altimeter System (GLAS) provides continent-wide imagery of the vertical structure of Antarctic cloudiness, but results based on GLAS over Antarctica were published for only one calendar month (October 2003, Spinhirne et al. 2005). Spaceborne Cloud–Aerosol Lidar and Infrared Pathfinder Satellite Observation (CALIPSO) satellite measurements have been used to examine clouds over Antarctica, but primarily at stratospheric levels (e.g., Noel et al. 2008; Wang and Sassen 2007).

The purpose of this contribution is to document for the first time the seasonally varying vertical structure of cloudiness throughout Antarctica and the high-latitude Southern Ocean. The study is made possible by the availability of three years of data from the *CloudSat* and CALIPSO satellites, which provide the most comprehensive observations available to date of the vertically varying distribution of clouds throughout the globe. The data provide an unprecedented opportunity to examine the distribution of clouds over a region of the world where the three-dimensional structure of the seasonal cycle remains largely unknown.

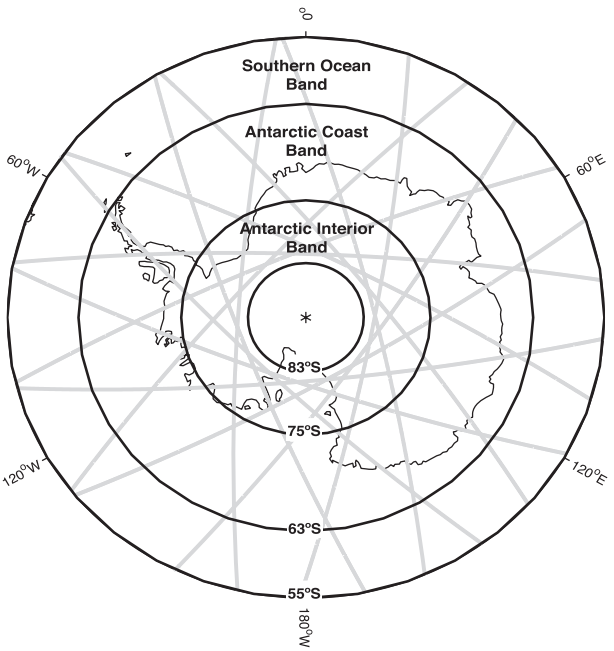

FIG. 1. The domain examined in this study. The black lines indicate the latitude bands considered in Figs. 2–4, hereafter denoted the Southern Ocean, Antarctic coast, and Antarctic interior bands. The gray lines indicate that the A-Train satellite passes over the Antarctic during a sample day.

2. Data and methods

The results are based on a combination of data from the *CloudSat* Cloud Profiling Radar (CPR) and the CALIPSO Cloud-Aerosol Lidar with Orthogonal Polarization (CALIOP). The information from the CPR and CALIOP instruments is combined to form the Radar–Lidar Geometric Profile Product (e.g., Mace et al. 2009), which provides information about the horizontal and vertical distribution of hydrometeors in the atmosphere from the surface to the stratosphere. Details regarding the CPR and CALIOP instruments and the resulting data products can be found online (at http://cloudsat.atmos.colostate.edu).

Results are based on 36 months of data from December 2006 to November 2009. The principal results are shown as ''cloud incidence'' averaged over select regions of the atmosphere. Area averaged cloud incidence was determined as follows.

1) On any given day, the *CloudSat* and CALIPSO satellites orbit the Earth roughly 14.5 times per day. The gray lines in Fig. 1 indicate the resulting distribution of satellite tracks over Antarctica summed over a randomly chosen day.
2) For each satellite track, the approximate cross-track footprint of the CPR is ~1.4 km, the along-track resolution is ~1.7 km, and the vertical sampling is at ~250 m. Each track can thus be decomposed into a series of volumes that are 1.4 km × 1.7 km in the horizontal and 250 m the vertical. On any given day, the tracks indicated in Fig. 1 correspond to upward of 12 800 000 individual data volumes, all of which are centered at a specific latitude, longitude, and vertical level over the high latitudes of the Southern Hemisphere.
3) The Radar–Lidar Geometric Profile Product [2B-Geoprof-lidar, see Stephens et al. (2008) for a review of all *CloudSat* products] provides estimates of cloud fraction within each 1.4 km × 1.7 km × 250 m volume as a percentage from 0% to 100%. If a given volume has a cloud fraction greater than 50%, we assign that volume a ''1''; otherwise, that volume is assigned a ''0'' (a similar threshold has been used in previous studies; e.g., Walden et al. 2003). Note that the scales of interest investigated here include thousands of atmospheric volumes sampled by the Radar–Lidar Geometric Profile Product. The large ''scale of interest'' to ''volume size'' ratio obviates the likelihood that the ''all or nothing'' approach will introduce spurious bias into the results.
4) We then average the binary cloud fraction data as a function of vertical level over a given latitude/longitude box and month. The resulting numerical values are thus indicative of cloud incidence as a function of vertical level. For example, if we want to calculate cloud incidence within a box extending from 72° to 83°S,

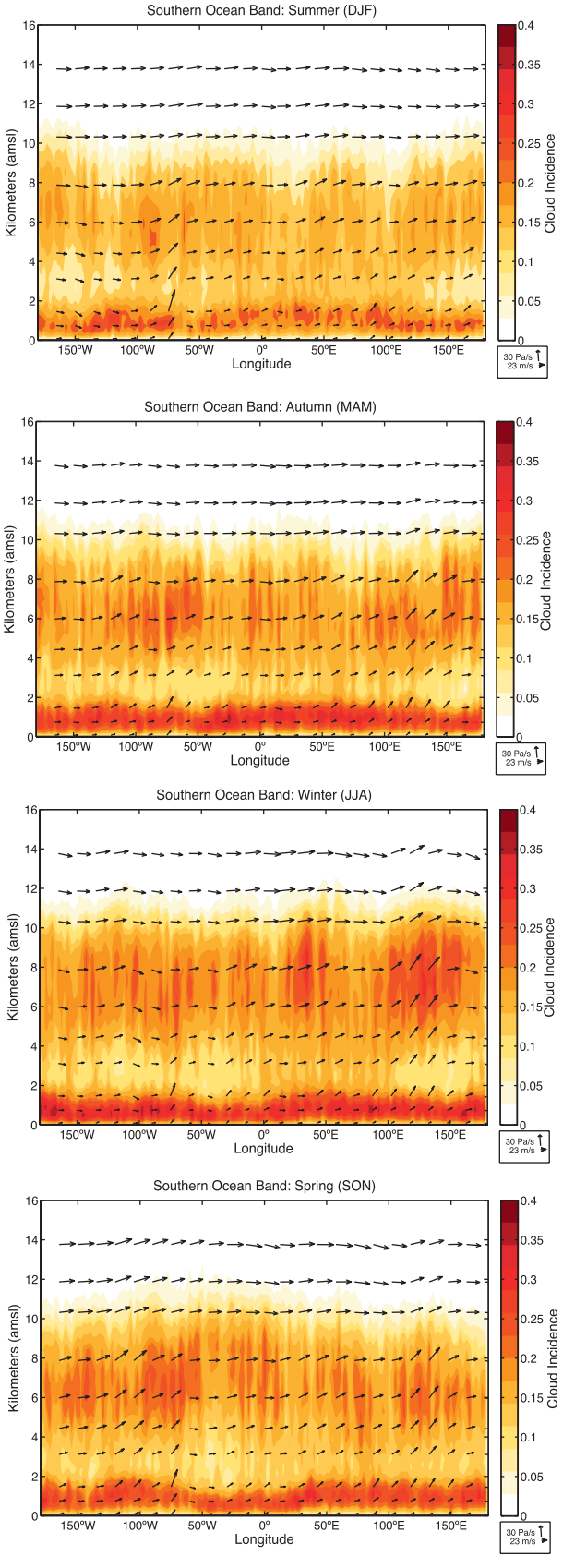

10° to 130°E during the month of January 2007, we average as a function of vertical level all volumes available during that month and latitude/longitude range. A cloud incidence of 0.4 at 6 km would thus indicate that during January 2007 a cloud was observed 40% of the time at 6 km within the area spanned by 72°–83°S, 10°–130°E.

Note that the results are shown in terms of cloud incidence rather than ice/liquid water content for two reasons: 1) the radar–lidar product used here provides estimates of cloud occurrence above a threshold, not water content, and 2) the conversion from cloud occurrence to ice water content is marked by numerous uncertainties (e.g., Wu et al. 2009).

For select figures, we also use 1) temperature data from the *CloudSat* European Centre for Medium-Range Weather Forecasts (ECMWF) Auxiliary Data product, which contains ECMWF forecast data interpolated to the same volumes sampled by the *CloudSat* cloud profiling radar, and 2) monthly mean wind data from the National Centers for Environmental Prediction (NCEP)–National Center for Atmospheric Research (NCAR) reanalysis dataset averaged over the same months used to derive the cloud incidence. The NCEP–NCAR reanalysis was obtained from the NOAA Physical Sciences Division.

3. Results

The seasonal cycle of cloudiness over the high latitudes of the Southern Hemisphere is presented in two types of figures: longitude–height profiles of cloud incidence averaged over a range of latitudes and vertical profiles of cloud incidence averaged over select latitude/longitude boxes. We first examine longitude–height profiles of cloud incidence for the three latitude bands indicated in Fig. 1: the Southern Ocean band (55°–63°S), the Antarctic coast band (63°–75°S), and the Antarctic interior band (75°–83°S). The longitude–height profiles found by averaging all three years of data are shown in Figs. 2–4. Results for individual 12-month periods are shown in the appendix, Figs. A1–A3.

Figure 2 shows longitude–height profiles of cloud incidence for the Southern Ocean latitude band for the

←

FIG. 2. Vertical profiles of cloud incidence over the Southern Ocean latitude band for the seasons indicated. Cloud incidence (defined in the text) provides an approximate measure of the incidence of clouds within a given atmospheric volume. The arrows indicate the corresponding monthly-mean wind direction and velocity. Results for individual years are presented in the appendix.

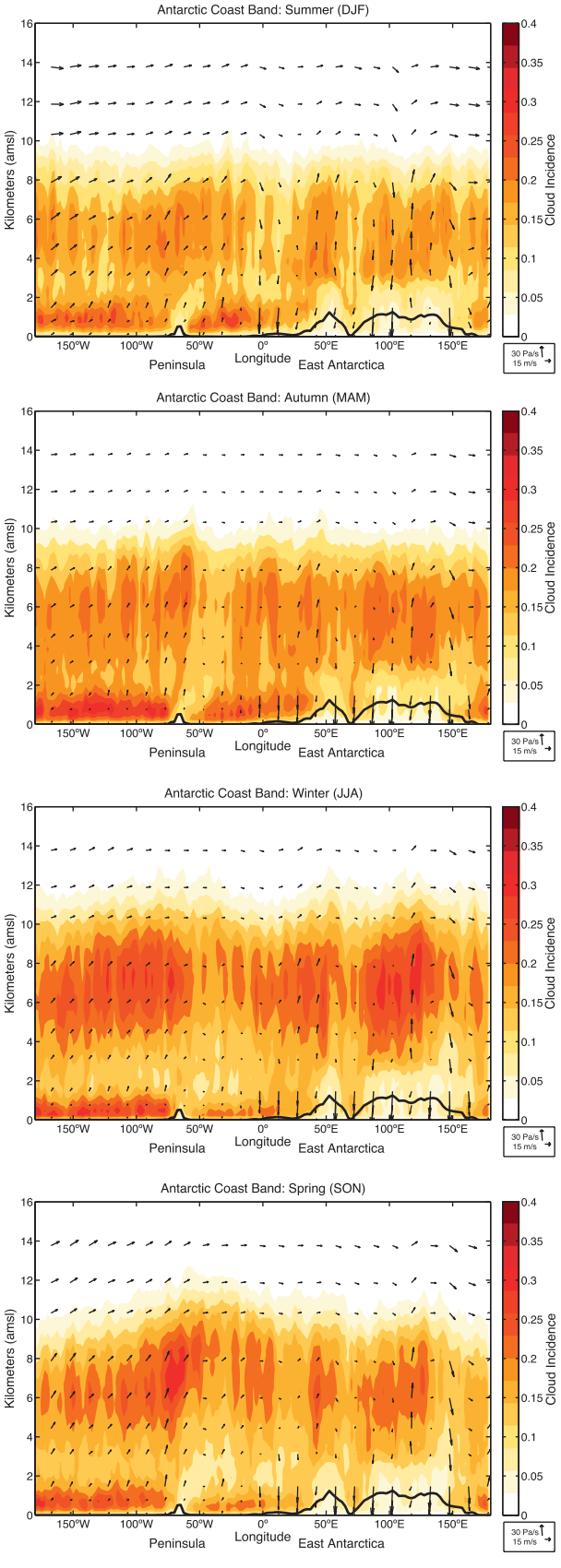

(top to bottom) austral summer, autumn, winter, and spring seasons. In all figures, shading denotes mean cloud incidence and the vectors denote the mean wind field for the coincident months from the NCEP–NCAR reanalysis. Cloud incidence over the Southern Ocean exhibits two distinct maxima: one centered near the surface (below 2 km) and another centered in the upper troposphere (~6–8 km). The lower maximum is consistent with a persistent layer of low stratiform clouds over the high-latitude Southern Ocean (e.g., Klein and Hartmann 1993) and has largest amplitude during autumn and winter; the upper maximum likely reflects clouds associated with extratropical cyclones and exhibits largest amplitude during winter. In general, there is little east–west structure in cloud incidence over the Southern Ocean. However, cloud incidence exhibits a slight peak near ~130°E in the upper troposphere during winter, and this peak is coincident with a region of enhanced vertical motion in the wind field. The collocation of the maxima in vertical velocity and cloud incidence lends credence to the reliability of both features.

The dominant features in Fig. 2 are also generally evident in individual years (see Fig. A1). The interannual variability in the Southern Ocean region is dominated by a wintertime peak in cloudiness in 2009 and a slightly less pronounced summertime peak in cloudiness during 2007. Note that in both the mean maps (Fig. 2) and the maps for individual years (Fig. A1), there is strong correspondence between regions of enhanced vertical motion and relatively high cloud incidence.

Figure 3 shows analogous results for the Antarctic coast band. The coastal band is dominated by ocean to the west of the prime meridian but by land to the east of it (the area averaged surface elevation is indicated by the thick black line at the bottom of the panels). As is the case over much of the Southern Ocean (Fig. 2), the coastal regions to the west of 0° longitude are marked by two maxima in cloud incidence: a maximum near the surface consistent with low stratiform clouds and a maximum in the upper troposphere. The low stratiform clouds have largest amplitude during autumn and winter, are restricted to ocean areas of the plot, and are notably interrupted by the Antarctic Peninsula. Upper-level cloudiness is relatively uniform over the ocean and

←

FIG. 3. As in Fig. 2 but for the Antarctic Coast band, as indicated in Fig. 1. The thick black line near the bottom of all panels is the meridionally averaged surface elevation. Note that the cloud incidence scaling is the same as in Fig. 2, but the vector scaling is different from that in Fig. 2.

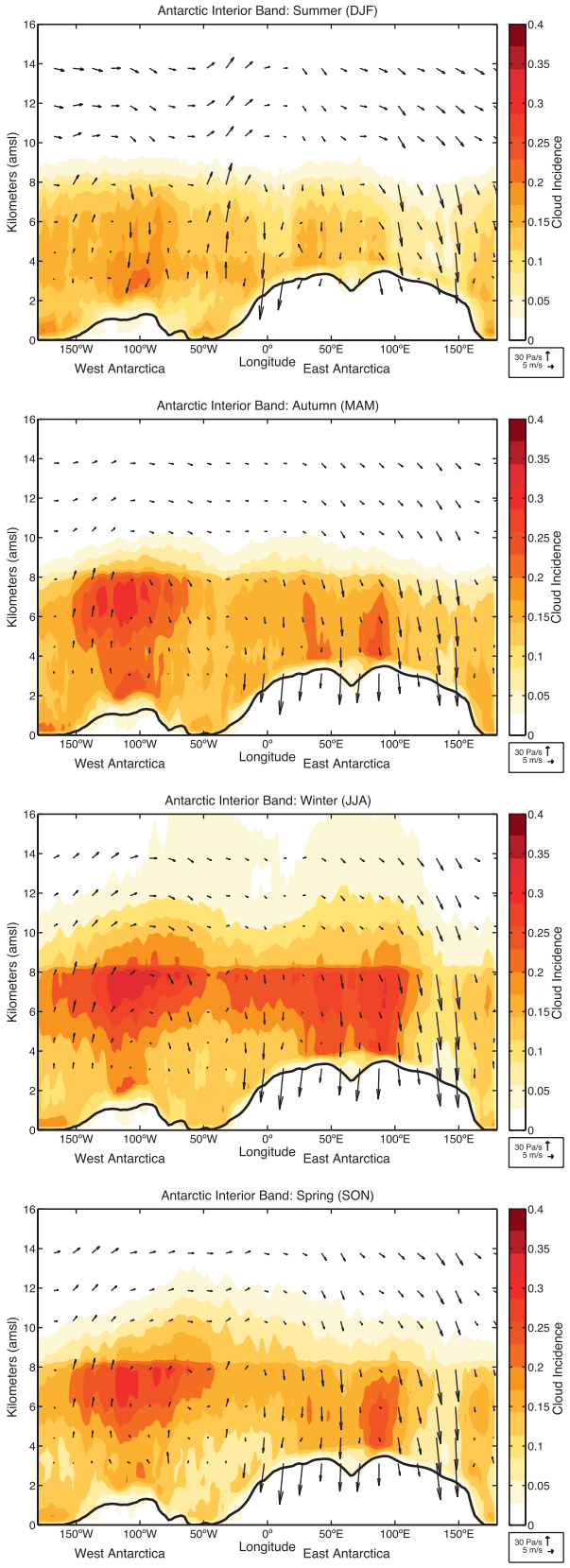

FIG. 4. As in Fig. 3 but for the Antarctic Interior band, as indicated in Fig. 1.

land areas but peaks notably upwind of the Antarctic Peninsula (i.e., west of ~70°W). Over most longitudes, upper-level cloud incidence is lowest during the summer and highest during winter and spring. Cloud incidence also exhibits a marked bowed structure upwind of the peninsula, which is most notable during spring (between 100° and 50°W) and is consistent with enhanced vertical motion in this region. The primary features evident in Fig. 3 are generally apparent in individual years (see Fig. A2). The most pronounced aspects of the interannual variability are that 1) the bowed structure upwind of the Peninsula is most readily apparent in 2007 and 2008 and 2), as is the case over the Southern Ocean, cloud incidence exhibits relatively high summertime values during 2007 and relatively high wintertime values during 2009.

Figure 4 shows cloud incidence for the southernmost band, which covers much of the Antarctic interior (see Fig. 1). Cloud incidence over the interior exhibits a very different structure than that found over other latitude bands. In general, cloud incidence is lowest during summer and highest during winter. A similar seasonal cycle over the high latitudes of the Southern Hemisphere is evident in the AVHRR data and ISCPP datasets (e.g., Hatzianastassiou et al. 2001; Pavolonis and Key 2003; Town et al. 2007) and, as evidenced in Fig. 4, the seasonal cycle is particularly pronounced over the regions of highest terrain (e.g., over western and eastern Antarctica). The most notable features in cloud incidence over the interior of Antarctica include (i) relatively low cloud incidence over West and East Antarctica during summer, (ii) a sharp drop-off in cloud incidence near 8 km over much of the continent that is most pronounced during autumn, winter, and spring, and (iii) widespread cloudiness at stratospheric levels during winter and spring, consistent with the seasonality of polar stratospheric clouds (PSCs) (e.g., McCormick and Trepte 1986; Poole and Pitts 1994). As in Figs. 2 and 3, there is generally good agreement between the fields of vertical motion and cloud incidence; that is, the region of low cloud incidence on the eastern slope of East Antarctica is coincident with locally large subsidence there. The key features listed above are all readily apparent in individual years (Fig. A3).

Several primary aspects of high-latitude Southern Hemisphere cloudiness are also revealed in vertical profiles of cloud incidence averaged over four regions of Antarctica: the Antarctic Peninsula (Fig. 5a), West Antarctica (Fig. 5b), a representative section of the Southern Ocean (Fig. 5c), and the East Antarctic Plateau (Fig. 5d). The results in Fig. 5 clearly indicate the following:

1) the existence of two distinct maxima in vertical profiles of cloud incidence over ocean areas (Figs. 5a,c)

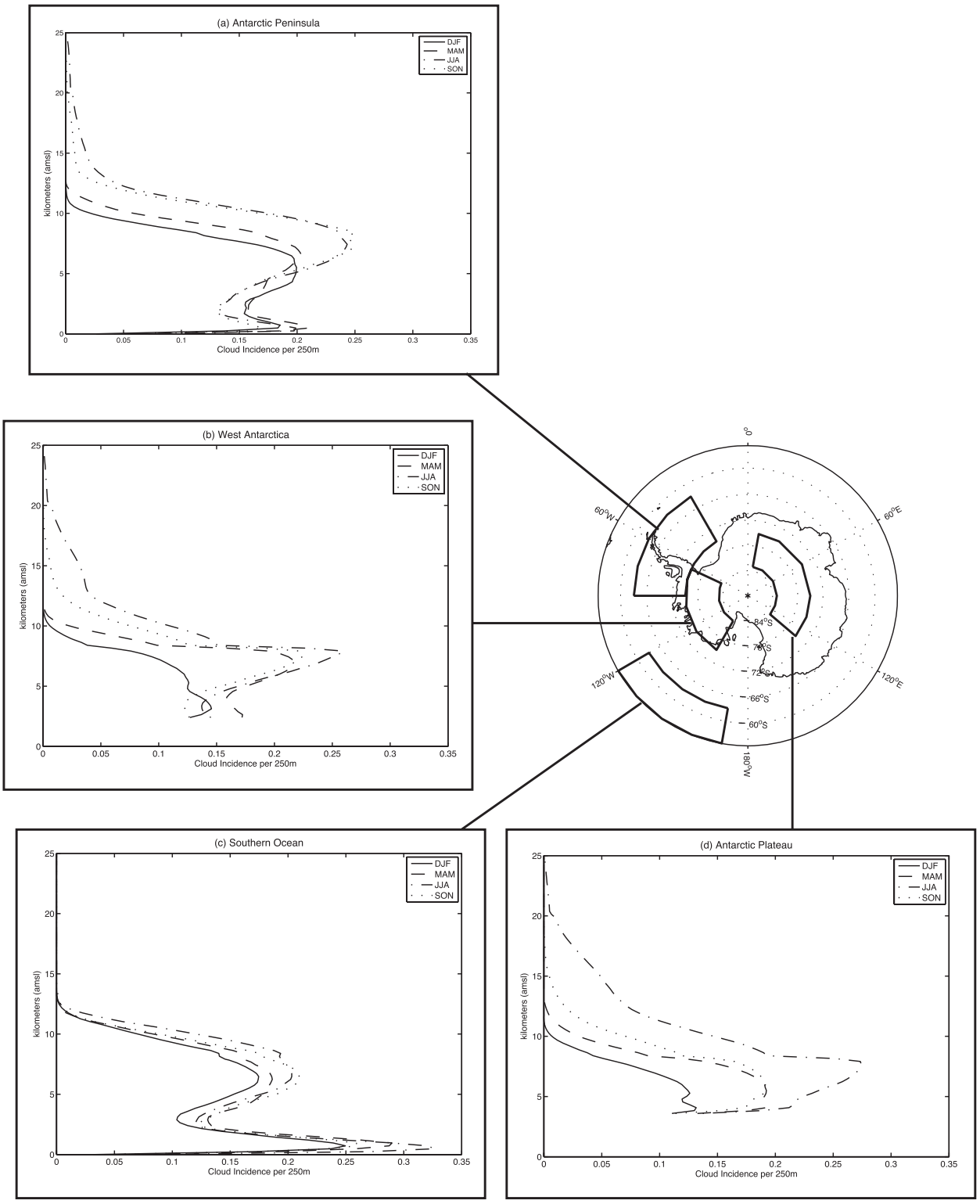

FIG. 5. Cloud incidence averaged over the four regions indicated in the map. Panels show results for (a) the Antarctic Peninsula, (b) West Antarctica, (c) the Southern Ocean, and (d) the Antarctic Plateau. In all panels, results for summer are indicated as solid lines, autumn as dashed lines, winter as dashed–dotted lines, and spring as dotted lines.

and the summertime minimum in cloud incidence over the Southern Ocean (Fig. 5c);
2) the summertime minimum in cloudiness at upper levels over East Antarctica, West Antarctica, and the peninsula region (Figs. 5a,b,d);
3) the sharp drop-off in cloud incidence ~8 km over the Antarctic ice sheet (Figs. 5b,d; the discontinuity is particularly pronounced during the cold season months over West Antarctica); and
4) the extension of clouds to stratospheric levels during winter over the continental areas (Figs. 5a,b,d). As discussed further in section 4, mean cloud incidence is characterized not by a secondary maximum at stratospheric levels but by monotonically decreasing cloud incidence from the tropopause level to ~20 km.

4. Discussion

The results in Figs. 2–5 document for the first time the seasonally varying vertical structure of cloudiness throughout the Southern Hemisphere high latitudes. The results highlight several key features of Antarctic cloudiness, and they provide a baseline of Southern Hemisphere high-latitude cloudiness for future observational and modeling studies.

Among the most robust results is the seasonal cycle in cloudiness throughout the high latitudes of the Southern Hemisphere, with lowest cloud incidences generally found during the summer season over all regions. The summertime minimum in cloudiness over the Southern Ocean (Fig. 2) is consistent with the seasonal cycle in extratropical cyclone activity, but it is less clear what gives rise to the pronounced summertime minimum in cloudiness over the continent. One explanation is that the seasonal cycle in tropospheric cloudiness over the continent is driven by the advection of clouds and moisture from the Southern Ocean region. Since cloudiness peaks over the Southern Ocean during the cold season months, it follows that there is a larger source of cloudiness available for advection over Antarctica during these seasons as well. Another explanation is that the summertime minimum is driven by the seasonal cycle in saturation vapor pressures over Antarctica. For example, an ~10 K increase in temperatures from, say, ~200 to ~210 K results in nearly a threefold increase in the saturation vapor pressure over ice. Thus, water vapor advected from the Southern Ocean region will more readily condense over the continent during the cold season months than the summer season. It is unclear why the seasonal cycle in Antarctic cloud incidence exhibits largest amplitude over the high terrain of West and East Antarctica (Fig. 4).

Another intriguing result is the appearance of two distinct maxima in cloud incidence over the Southern Ocean: one in the boundary layer and another at upper tropospheric levels (Figs. 2 and 5c). Both features are consistent with the associated profiles of static stability. For example, Fig. 6 shows the vertical profiles of wintertime cloud incidence from Fig. 5 (dashed lines) superimposed on the associated vertical profiles of the static stability (solid lines). The potential temperature data are derived from the ECMWF auxiliary data and static stability is defined as $\theta^{-1}d\theta/dz$ in which θ is the potential temperature. The corresponding profiles of wintertime temperatures are shown in Fig. 7. As evident in Fig. 6c, the low-level maximum in cloud incidence over the Southern Ocean is centered immediately below a low-level maximum in lower tropospheric static stability. Hence, the low-level maximum in Southern Ocean cloud incidence is consistent with widespread low stratiform clouds trapped below the inversion at the top of the atmospheric boundary layer (see also Klein and Hartmann 1993). The upper-level maximum in cloud incidence peaks just above the tropospheric minimum in static stability (as indicated by the black horizontal line). Thus, upper tropospheric cloudiness peaks immediately above the least stable region of the atmosphere.

Several features revealed in Figs. 2–6 are more difficult to interpret. The near-discontinuous drop-off in wintertime cloud incidence over the interior of Antarctica near ~8 km (Figs. 4 and 5) is not due to any known biases in the instruments aboard *CloudSat* and is a seemingly robust feature of Antarctic climate. A sharp vertical gradient in long-term mean cloudiness might be expected in regions where the static stability is very high, or where the height of the tropopause fluctuates relatively little from day to day (and thus where long-term averages do not smear out the height of the tropopause). However, the drop-off is not clearly linked to profiles of static stability (Figs. 6b,d). Also, the day-to-day variance in the height of the tropopause is just as large over the continent as it is over the Southern Ocean region (i.e., where cloud incidence exhibits a much smoother vertical profile; variance not shown).

Another mysterious result is the seasonal cycle in upper-level cloud incidence in the region upwind of the Antarctic Peninsula (Fig. 3). The large east–west gradients in upper-level cloudiness in the vicinity of the Antarctic Peninsula are consistent with rising motion forced by the Antarctic Andes (Fig. 3, vectors). But, it is not clear why both the rising motion and east–west bowed structure peak so clearly during the spring season (Fig. 3, bottom).

Several of the results shown here are consistent with findings reported in previous studies. The increases in

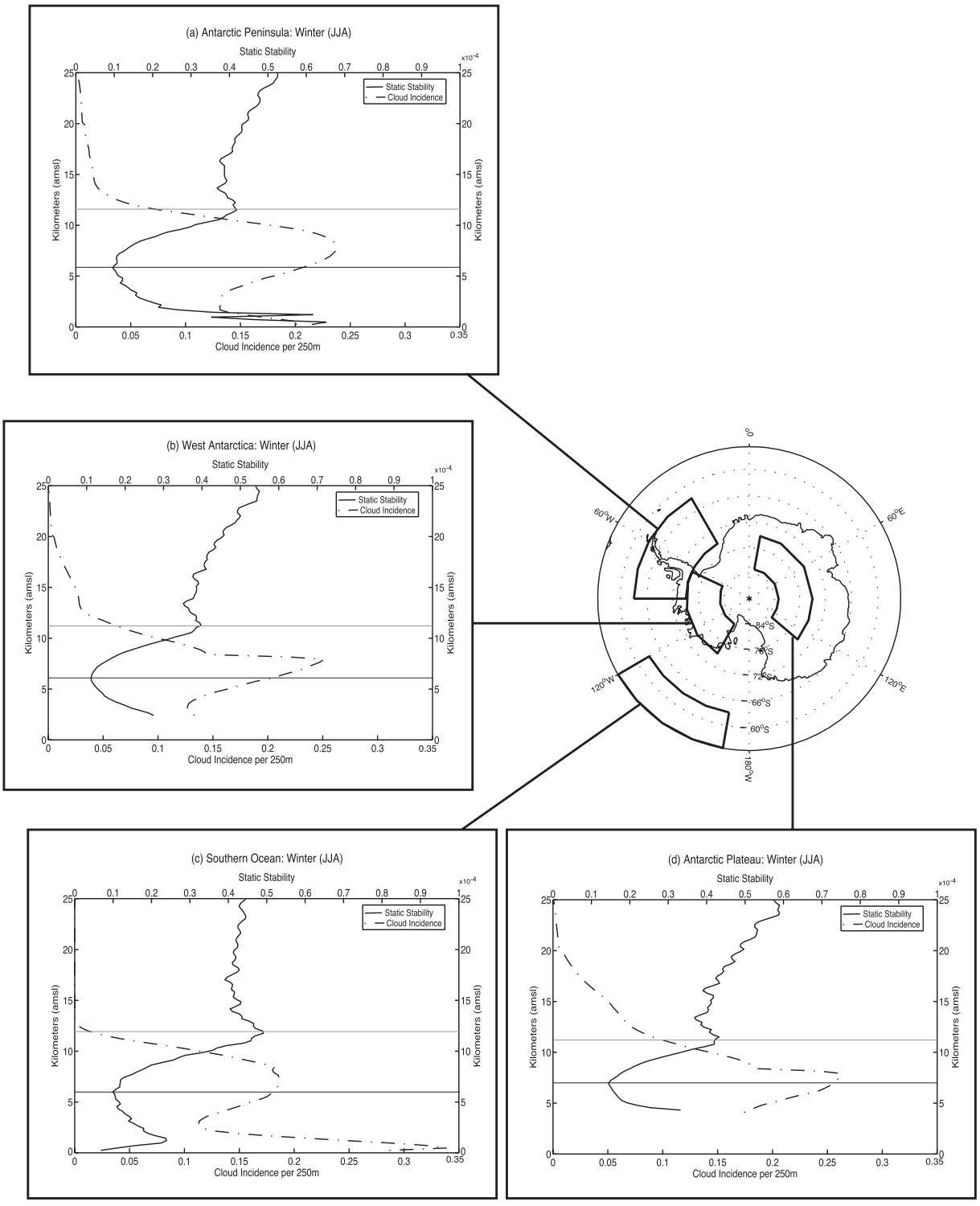

FIG. 6. As in Fig. 5 but dashed–dotted lines indicate cloud incidence during winter (reproduced from Fig. 5), and solid lines indicate the corresponding profiles of static stability. In all panels, the black horizontal line indicates the upper tropospheric minimum in static stability and the gray horizontal line indicates the level at which static stability has a local lower stratospheric maximum.

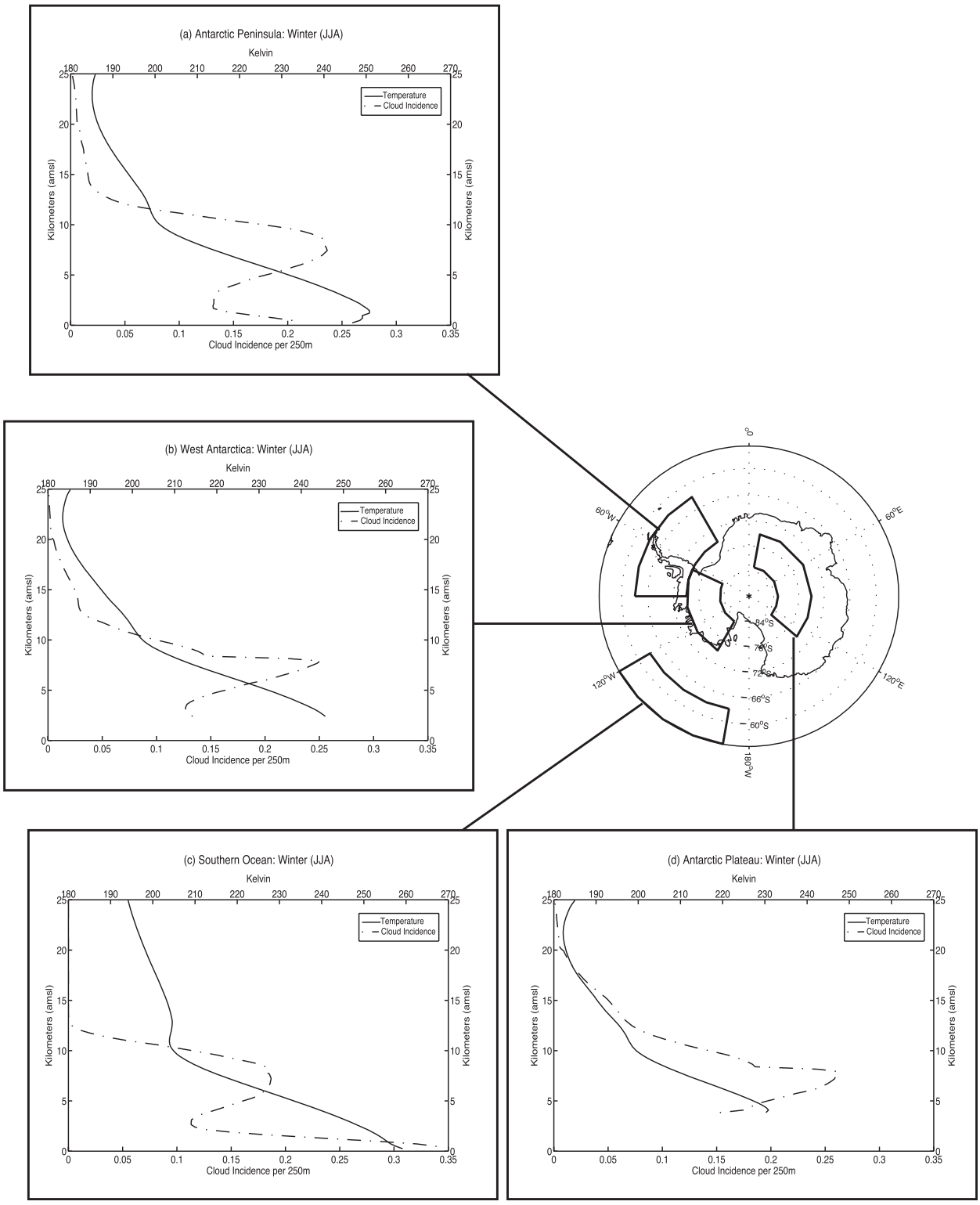

FIG. 7. As in Fig. 5 but the dashed–dotted lines indicate cloud incidence during winter (reproduced from Fig. 5), and solid lines indicate the corresponding profiles of temperature (K).

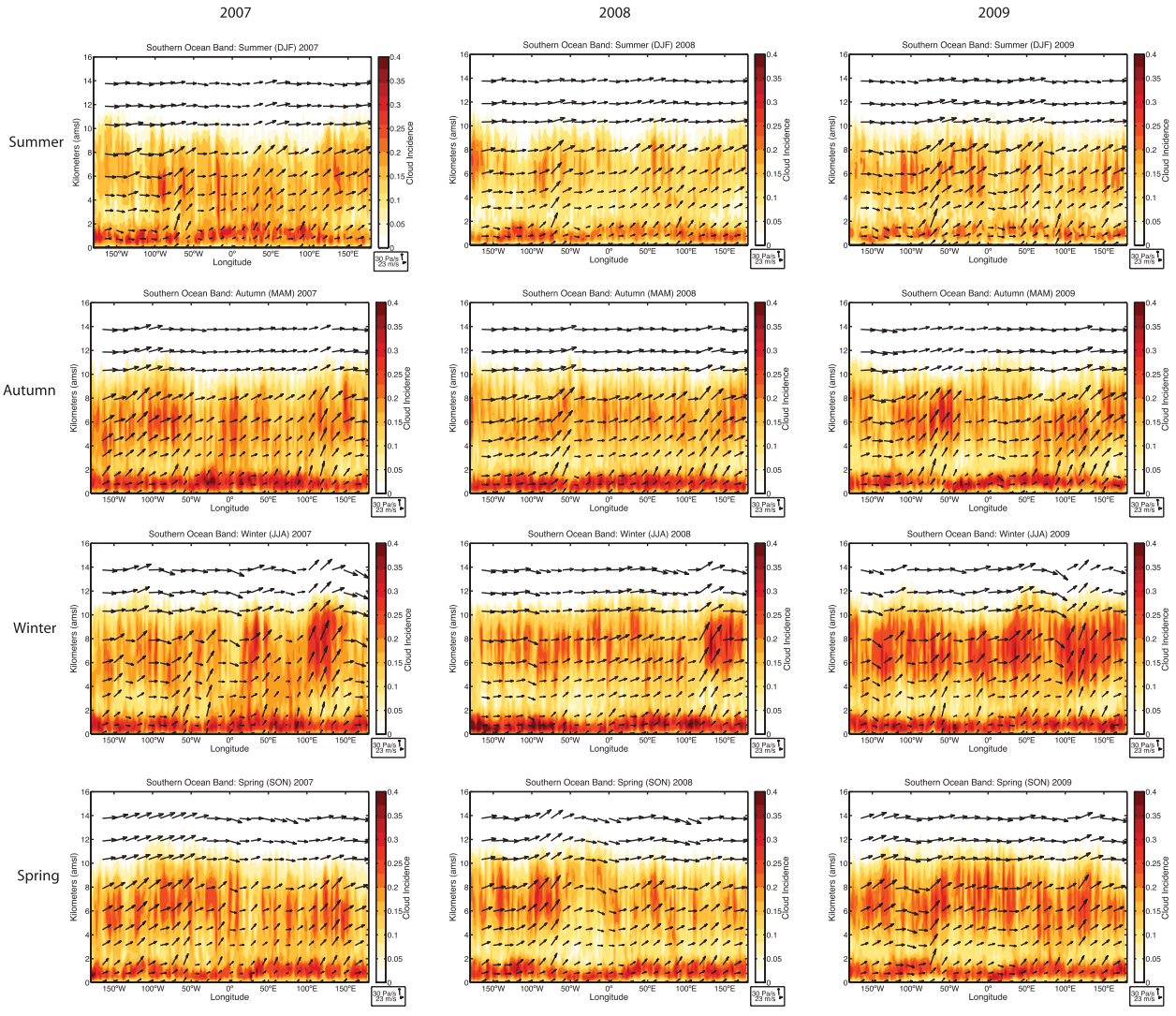

FIG. A1. As in Fig. 2 but for vertical profiles of cloud incidence over the Southern Ocean latitude band for the seasons indicated, broken down by year, for (left) 2007, (middle) 2008, and (right) 2009. Cloud incidence (defined in the text) provides an approximate measure of the incidence of clouds within a given atmospheric volume. The arrows show wind direction and velocity.

cloudiness over the plateau during winter detected by *CloudSat* and CALIPSO are consistent with the seasonal cycle of polar cloudiness inferred from AVHRR (Polar Pathfinder) data and the ISCCP dataset (Murata and Yamanouchi 1997; Hatzianastassiou et al. 2001, cf. Figs. 2 and 3; Pavolonis and Key 2003, cf. Fig. 2; Town et al. 2007). The weak seasonal cycle over the Antarctic coast and Southern Ocean presented here also agrees well with findings based on AVHRR data and the ISCCP dataset (e.g., Murata and Yamanouchi 1997; Hatzianastassiou et al. 2001, cf. Figs. 2 and 3; Pavolonis and Key 2003, cf. Fig. 2). The distinctly larger cloud fraction on the west side of the peninsula as compared to the east side (particularly through the 4–8-km layer) is consistent with the findings of Turner et al. (2001) from AVHRR data.

We have focused primarily on clouds at tropospheric levels. However, the vertical structure of cloud incidence at stratospheric levels over the continent (e.g., Fig. 5) warrants further mention. The vertical structure suggests that long-term mean wintertime cloudiness over the continent does not exhibit a secondary maximum at stratospheric levels, as suggested by vertical profiles of individual polar stratospheric clouds (e.g., Solomon 1999, cf. Fig. 5; Noel et al. 2008, cf. Fig. 1) or the vertical profile of polar stratospheric clouds derived from the Stratospheric Aerosol Measurement (SAM II) sensor (McCormick and Trepte 1986, cf. Fig. 1; Poole and Pitts 1994, cf. Fig. 2). Rather, it suggests that cloudiness decreases monotonically from the tropopause to at least 20 km. The differences between the vertical profiles of clouds at

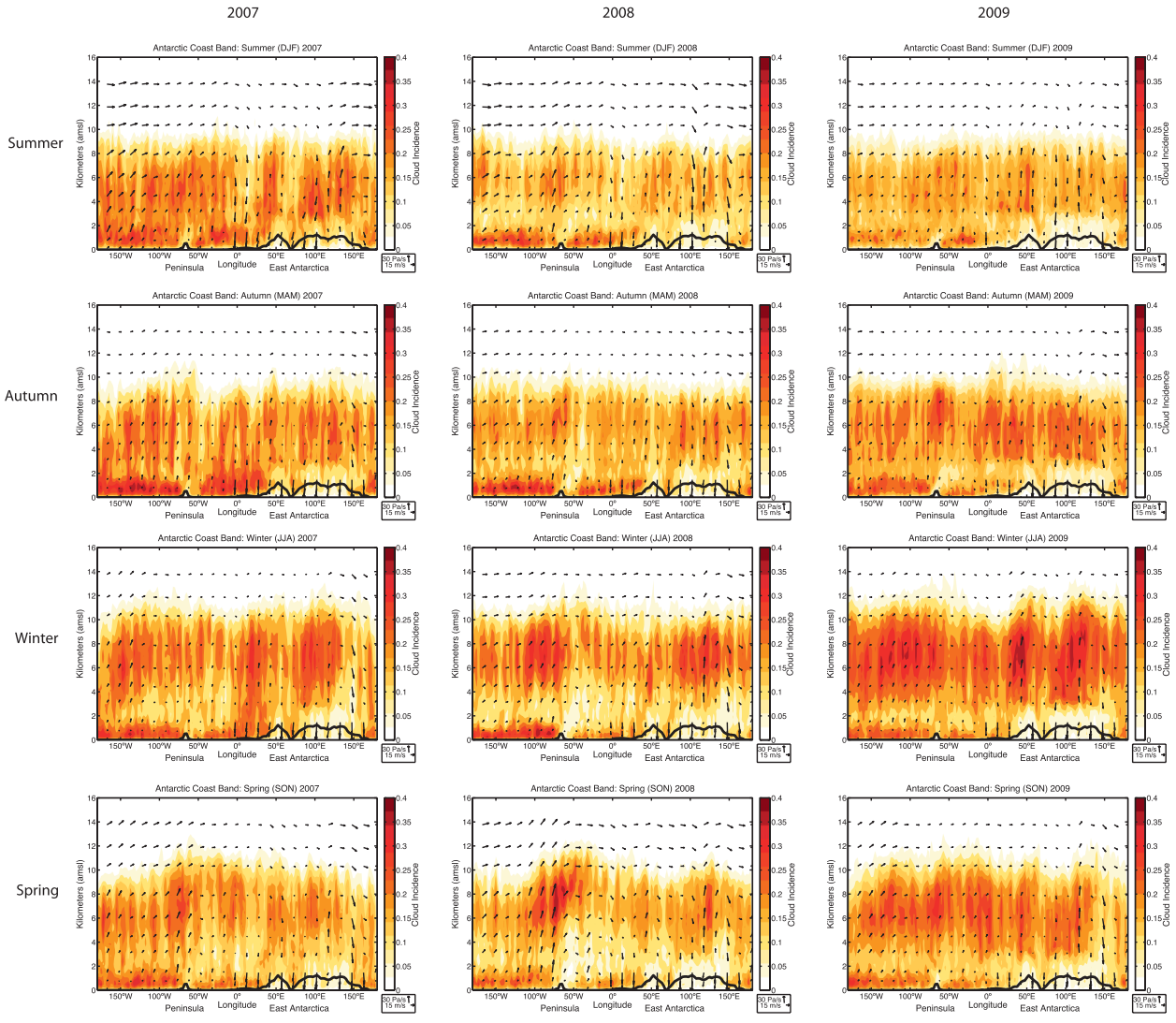

FIG. A2. As in Fig. A1 but for the Antarctic coast band. The thick black line near the bottom of all panels is the meridionally averaged surface elevation.

stratospheric levels revealed here and in prior studies may be due to sampling variability; for example, individual clouds are not necessarily indicative of the long-term mean): the SAM II sensor measures polar stratospheric clouds via attenuated sunlight through the earth's limb and does not sample polar night.

A possible physical reason for the near-monotonic decrease in clouds above the tropopause is that a component of cloudiness at lower stratospheric levels derives from mixing with the troposphere (e.g., Wang and Sassen 2007). A similar conclusion is suggested by the vertical profiles of static stability and cloud incidence. For example, the absence of clouds in the lowermost stratosphere over the Southern Ocean is consistent with temperatures higher than the ~200 K threshold for PSC formation (Fig. 7c), but it is also consistent with the relatively high values of static stability at the midlatitude tropopause (Fig. 6c). Similarly, the presence of clouds in the lowermost stratosphere over the continent is consistent with temperatures lower than ~200 K (Figs. 7a,b,d), but it is also consistent with the relatively weak values of static stability at the polar tropopause (Figs. 6a,b,d). Thus, while it is clear that PSC formation depends critically on stratospheric temperatures (e.g., McCormick and Trepte 1986; Poole and Pitts 1994; Solomon 1999), the vertical profiles of cloudiness and static stability shown in Fig. 7 suggest that cloudiness in the lowermost stratosphere may also be affected by mixing with tropospheric levels.

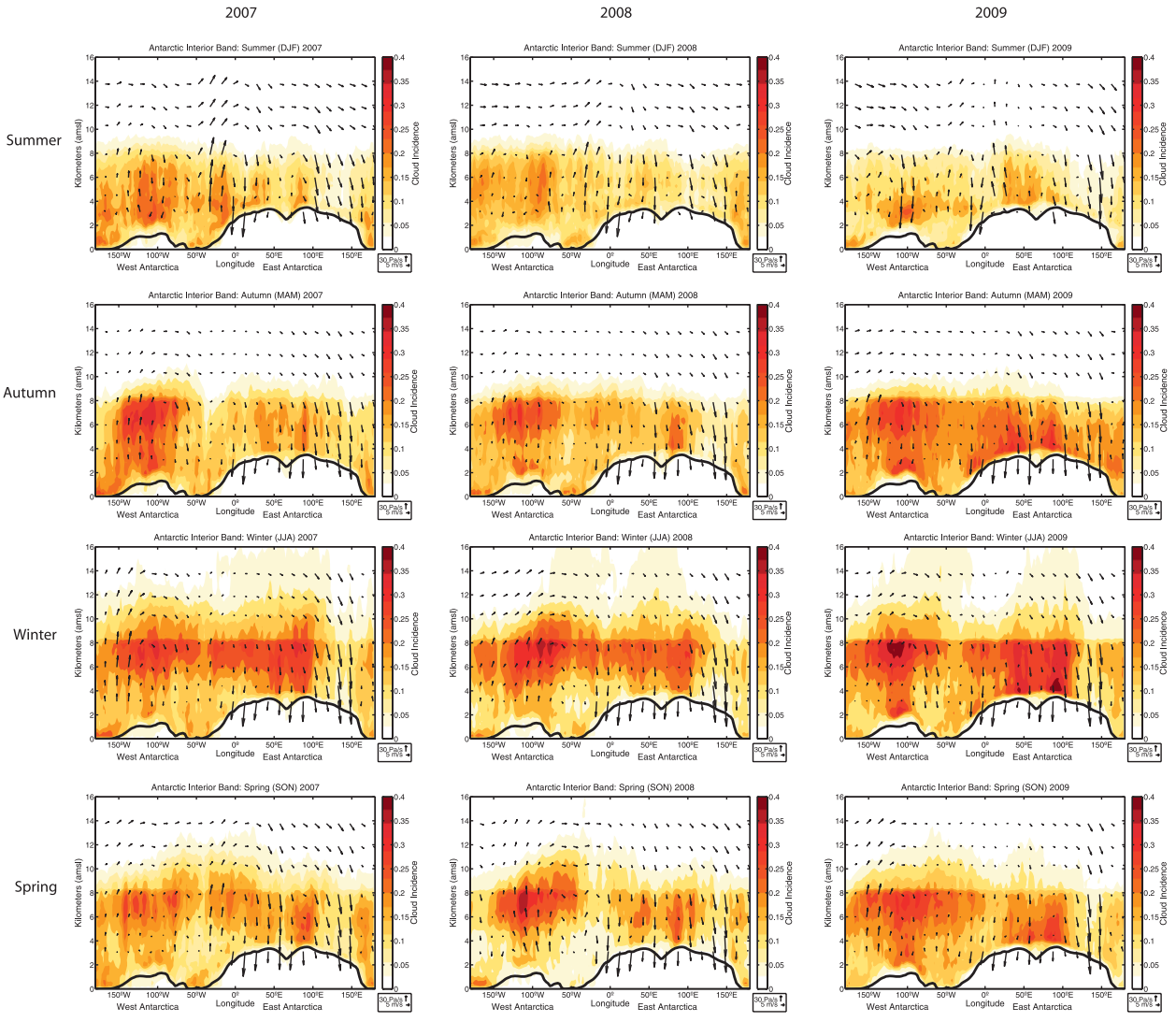

FIG. A3. As in Fig. A2 but for the Antarctic interior band.

Acknowledgments. The results in this paper are an outgrowth of KLV's master's thesis in the Department of Atmospheric Science at Colorado State University. KLV and DWJT were supported by the National Science Foundation Grant AMT-0613082. KLV was supported under the NASA Award NAS5-99237 during the final year of her degree. GLS was supported under the NASA Award NNX07AR11G.

APPENDIX

Cloud Incidence in Individual Years

The cloud incidence for individual years is shown for the Southern Ocean in Fig. A1, the Antarctic coastal band in Fig. A2, and Antarctic interior in Fig. A3.

REFERENCES

Hatzianastassiou, N., N. Cleridou, and I. Vardavas, 2001: Polar cloud climatologies from ISCCP C2 and D2 datasets. *J. Climate,* **14,** 3851–3862.

Kay, J. E., T. L'Ecuyer, A. Gettelman, G. L. Stephens, and C. O'Dell, 2008: The contribution of cloud and radiation anomalies to the 2007 Arctic sea ice extent minimum. *Geophys. Res. Lett.,* **35,** L08503, doi:10.1029/2008GL033451.

Klein, S. A., and D. L. Hartmann, 1993: The seasonal cycle of low stratiform clouds. *J. Climate,* **6,** 1587–1606.

Lachlan-Cope, T., R. Ladkin, J. Turner, and P. Davison, 2001: Observations of cloud and precipitation particles on the Avery Plateau, Antarctic Peninsula. *Antarct. Sci.,* **13,** 329–348.

Lubin, D., and D. A. Harper, 1996: Cloud radiative properties over the South Pole from AVHRR infrared data. *J. Climate,* **9,** 3405–3418.

Mace, G. G., Q. Zhang, M. Vaughn, R. Marchand, G. Stephens, C. Trepte, and D. Winker, 2009: A description of hydrometeor

layer occurrence statistics derived from the first year of merged CloudSat and CALIPSO data. *J. Geophys. Res.,* **114,** D00A26, doi:10.1029/2007JD009755.

Mahesh, A., V. P. Walden, and S. G. Warren, 2001: Ground-based infrared remote sensing of cloud properties over the Antarctic Plateau. Part I: Cloud-base heights. *J. Appl. Meteor.,* **40,** 1265–1278.

McCormick, M. P., and C. R. Trepte, 1986: SAM II measurements of Antarctic PSCs and aerosols. *Geophys. Res. Lett.,* **13,** 1276–1279.

Murata, A., and T. Yamanouchi, 1997: Distribution characteristics of clouds over East Antarctica in 1987 obtained from AVHRR. *J. Meteor. Soc. Japan,* **75,** 81–93.

Noel, V., A. Hertzog, H. Chepfer, and D. M. Winker, 2008: Polar stratospheric clouds over Antarctica from CALIPSO spaceborne lidar. *J. Geophys. Res.,* **113,** D02205, doi:10.1029/2007JD008616.

Pavolonis, M. J., and J. R. Key, 2003: Antarctic cloud radiative forcing at the surface estimated from the AVHRR Polar Pathfinder and ISCCP D1 datasets, 1985–93. *J. Appl. Meteor.,* **42,** 827–840.

Poole, L. R., and M. C. Pitts, 1994: Polar stratospheric cloud climatology based on Stratospheric Aerosol Measurement II observations from 1978 to 1989. *J. Geophys. Res.,* **99,** 13 083–13 089.

Solomon, S., 1999: Stratospheric ozone depletion: A review of concepts and history. *Rev. Geophys.,* **37,** 275–316.

Spinhirne, J. D., S. P. Palm, and W. D. Hart, 2005: Antarctica cloud cover for October 2003 from GLAS satellite lidar profiling. *Geophys. Res. Lett.,* **32,** L22S05, doi:10.1029/2005GL023782.

Stephens, G. L., and Coauthors, 2008: CloudSat mission: Performance and early science after the first year of operation. *J. Geophys. Res.,* **113,** D00A18, doi:10.1029/2008JD009982.

Town, M. S., V. P. Walden, and S. G. Warren, 2007: Cloud cover over the South Pole from visual observations, satellite retrievals, and surface-based infrared radiation measurements. *J. Climate,* **20,** 544–559.

Turner, J., G. J. Marshall, and R. S. Ladkin, 2001: An operational, real-time cloud detection scheme for use in the Antarctic based on AVHRR data. *Int. J. Remote Sens.,* **22,** 3027–3046.

Walden, V. P., S. G. Warren, and E. Tuttle, 2003: Atmospheric ice crystals over the Antarctic plateau in winter. *J. Appl. Meteor.,* **42,** 1391–1405.

Wang, Z., and K. Sassen, 2007: Level 2 cloud scenario classification product process description and interface control document, version 5.0. Cooperative Institute for Research in the Atmosphere, Colorado State University, 50 pp. [Available online at http://www.cloudsat.cira.colostate.edu/ICD/2B-CLDCLASS/2B-CLDCLASS_PDICD_5.0.pdf.]

Wu, D. L., and Coauthors, 2009: Comparisons of global cloud ice from MLS, CloudSat and correlative data sets. *J. Geophys. Res.,* **114,** D00A24, doi:10.1029/2008JD009946.

Yamanouchi, T., and S. Kawaguchi, 1992: Cloud distribution in the Antarctic from AVHRR data and radiation measurements at the surface. *Int. J. Remote Sens.,* **13,** 111–127.